Aging Brain 4 (2023) 100091

Contents lists available at ScienceDirect

Aging Brain

journal homepage: www.elsevier.com/locate/nbas

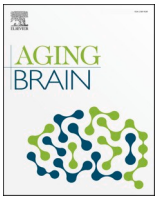

Sleep deprivation aggravated amyloid β oligomers-induced damage to the cerebellum of rats: Evidence from magnetic resonance imaging

Wensheng Guo [a,1], Xin Mao [a,1], Ding Han [a], Hongqi Wang [a], Wanning Zhang [a], Guitao Zhang [a], Ning Zhang [b], Binbin Nie [c], Hui Li [a], Yizhi Song [a], Yan Wu [a,*], Lirong Chang [a,*]

[a] *Department of Anatomy, School of Basic Medical Sciences, Beijing Key Laboratory of Neural Regeneration and Repair, Beijing Institute of Brain Disorders, Capital Medical University, Beijing, China*
[b] *Department of Neuropsychiatry and Behavioral Neurology and Clinical Psychology, China National Clinical Research Center for Neurological Diseases, Beijing Tiantan Hospital, Capital Medical University, Beijing, China*
[c] *Beijing Engineering Research Center of Radiographic Techniques and Equipment, Institute of High Energy Physics, Chinese Academy of Sciences, Beijing, China*

ARTICLE INFO

Keywords:
Alzheimer's disease
Amyloid-β oligomer
Sleep deprivation
Magnetic resonance imaging
Cerebellum

ABSTRACT

For quite a long time, researches on Alzheimer's disease (AD) primarily focused on the cortex and hippocampus, while the cerebellum has been ignored because of its abnormalities considered to appear in the late stage of AD. In recent years, increasing evidence suggest that the cerebellar pathological changes possibly occur in the preclinical phase of AD, which is also associated with sleep disorder. Sleep disturbance is a high risk factor of AD. However, the changes and roles of cerebellum has rarely been reported under conditions of AD accompanied with sleep disorders. In this study, using an amyloid-β oligomers (AβO)-induced rat model of AD subjected to sleep deprivation, combining with a 7.0 T animals structural magnetic resonance imaging (MRI), we assessed structural changes of cerebellum in MRI. Our results showed that sleep deprivation combined with AβO led to an increased FA value in the anterior lobe of cerebellum, decreased ADC value in the cerebellar lobes and cerebellar nuclei, and increased cerebellum volume. Besides that, sleep deprivation exacerbated the damage of AβO to the cerebellar structural network. This study demonstrated that sleep deprivation could aggravate the damage to cerebellum induced by AβO. The present findings provide supporting evidence for the involvement of cerebellum in the early pathology of AD and sleep loss. Our data would contribute to advancing the understanding of the mysterious role of cerebellum in AD and sleep disorders, as well as would be helpful for developing non-invasive MRI biomarkers for screening early AD patients with self-reported sleep disturbances.

* Corresponding authors.
E-mail addresses: yanwu@ccmu.edu.cn (Y. Wu), changlirong@ccmu.edu.cn (L. Chang).
[1] These authors contributed equally to this work.

https://doi.org/10.1016/j.nbas.2023.100091
Received 1 July 2023; Received in revised form 29 July 2023; Accepted 1 August 2023

Introduction

Alzheimer's disease (AD) is the most common neurodegenerative disease, characterized by progressive deterioration in cognitive function and changes in behavior and personality. The typical pathological features of AD include senile plaques formed by deposition of extracellular amyloid-β and neurofibrillary tangles consisting of intracellular hyperphosphorylated tau proteins [1]. Amounting research on AD primarily focused on the pathological changes in the cortex and hippocampus, while the cerebellum is generally considered to show abnormalities only in the late stage of AD. Therefore it's not surprising that the cerebellum has long been ignored in AD-related research. However, an increasing amount of evidence suggest that the cerebellar pathological changes possibly occur in the preclinical phase of AD [2–5]. A recent research using voxel-based morphometry (VBM) analysis method based on magnetic resonance imaging (MRI) found atrophy of gray matter in the lobules I-V and VI of the vermis and paravermis in patients with amnestic mild cognitive impairment (MCI), while AD patients showed involvement of the lobule VI and crus I in the hemisphere [6]. The increased soluble amyloid-β oligomers (AβO) have been found in the cerebellum of sporadic AD patients and the level of soluble oligomers is correlated with cognitive dysfunction [7]. A line of evidence suggest that the cerebellum may play enigmatic undisclosed critical roles in early phase of AD, which is also associated with sleep disruption [2]. Sleep disorder is a high risk factor of AD and certain sleep disorders presented with decreased cerebellum activity. The complaints of sleep disturbance are common in patients with cerebellar diseases [8]. Moreover, considerable evidence has confirmed the involvement of the cerebellum in regulating sleep-wakefulness transition [2,9]. Cerebellar dysfunction could lead to decreased non-rapid eye movement (NREM) sleep and increased rapid eye movement (REM) sleep duration time [10]. However, the changes and roles of cerebellum has rarely been reported under conditions of AD accompanied with sleep disorders.

In this study, using an AβO-induced rat model of AD subjected to intermittent sleep deprivation (SD), combining with a 7.0 T animals structural magnetic resonance imaging (MRI), we assessed structural changes of cerebellum in MRI. Our results demonstrated that sleep deprivation could aggravate AβO-induced damage to the cerebellum, manifested as an increased FA value in the cerebellar anterior lobe, decreased ADC value in the cerebellar lobes, increased cerebellum volume, as well as enhanced connectivity in bilateral superior cerebellar peduncle.

Material and methods

Animals

Adult male Sprague-Dawley rats (6–8 weeks old, 270 ± 20 g) were randomly divided into four groups: Control (Con), sleep deprivation (SD), AβO injection (Aβ), and sleep deprivation plus AβO injection (SA) (n = 18 rats/group). All the rats were housed in pathogen-free cages and maintained relatively constant environmental conditions with temperature of (22 ± 2) ℃, humidity of (55 ± 2%), and a constant light/dark cycle of 12 h/12 h. The experiment was approved by the ethical committee of Capital Medical University (Permit Number: AEEI-2020–180) and followed Chinese Guide for Laboratory Animals.

Sleep deprivation

Rats were placed into a restrictive cage (Instrument model: KW-BD, Nanjing Calvin Biotechnology Co. Ltd.) with a built-in bar capable of discontinuous gentle rotation to disturb sleep of rats. Sleep deprivation was conducted for 7 days from 8:30 am to 4:30 pm, with a periodical rotation of 30 min and a 30-minute rest alternately. Control rats were placed in a similar-sized cage but without the rotating bar.

Intracerebroventricular (ICV) injection of soluble $A\beta_{1\text{-}42}$ oligomers

Briefly, $A\beta_{1\text{-}42}$ peptide (AnaSpec) was dissolved in hexafluoroisopropanol (HFIP), evaporated for 30 min, and then diluted in 2 mM DMSO to 1 mM for use. Rats were anesthetized and then fixed on the stereotaxic apparatus (Alc-H shanghai), 2.2 μl of soluble $A\beta_{1\text{-}42}$ oligomer was slowly delivered via unilateral i.c.v. (AP, −0.8 mm from bregma; ML, 1.2 mm; DV, −4.0 mm) in 5 min, followed by a 10-minute wait. The bone window was sealed with gel plastic, and the skin was sutured after topical penicillin disinfection.

MRI acquisition

Magnetic resonance imaging (MRI) was performed on a 7.0 T magnetic scanner (Bruker, Bioclinscan 70/30, Germany) after cognitive assessments, with a 290 mT/m self-shielded gradient system (gradient coil, BGA20-S), a body coil for RF transmission (RT aperture of 31 cm) and a four-channel surface coil for signal reception (2.3 × 1.5 cm^2). After localization sequences, high-resolution fat-saturated T2-weighted 2D turbo spin-echo (TSE) sequences in coronal and axial orientation were performed, with time of repetition (TR) = 3300 ms, time of echo (TE) = 41 ms, flip angle (FA) = 90°, field of view (FOV) = 40 × 40 mm^2, matrix = 240 × 320, slice thickness (ST) = 0.8 mm, number of slices (NS) = 18, number of acquisitions (NA) = 2,for axial slices, and with TR = 2600 ms, TE = 41 ms, FA = 90°, FOV = 32 × 40 mm^2, matrix = 192 × 320; ST = 0.8 mm, NS = 16, NA = 1 for coronal slices. Subsequently, DTI were acquired with an axial two-shot spin-echo planar imaging (EPI) sequence with 20 gradients of coding direction: TR = 4500 ms, TE = 41 ms, ST = 1.0 mm, NS = 12, FOV = 34 × 40 mm^2, matrix = 108 × 128, NA = 2; the b-value used for the acquisition of the diffusion-weighted image in each direction was 800 s/mm^2, and an additional image with b0 = 0 s/mm^2 was acquired as the b-value reference

image. Above scanning without slice gap, and during scanning, respiratory rate was monitored and body temperature was maintained at 37 °C (±2 °C).

MRI data processing

Structural preprocessing and VBM analysis

The T2 images of rat brain were preprocessed and statistical analyzed using the spmratIHEP toolkit in SPM12 (Welcome Department of Cognitive Neurology, London, UK). All the structural images were preprocessed using the following steps. Firstly, the origin of each structural image was repositioned at D3V according to the template image in spmratIHEP. Then the images were segmented into gray matter (GM), white matter (WM) and CSF according to tissue probability maps (TPM), and standardized into the Paxinos and Watson space using DARTEL (diffeomorphic anatomical registration through exponentiated lie). The transformation matrix was saved in the Jacobian Determinant, and used for modulating the normalized WM and CSF images, named as WMV and CSFV images. The WMV and CSFV images were further smoothed by a Gaussian kernel of 4 mm (after zooming) full width at half-maximum (FWHM). These modulated images were used for voxel-wised morphological (VBM) analysis. The VBM was performed on the smoothed images based on the generalized linear (GLM) model in spmratIHEP toolkit. To identify the difference of WMV and CSFV between control (Con) and sleep deprivation (SD), AβO injection (Aβ), and sleep deprivation plus AβO injection (SA) groups. Two-sample *t*-tests were performed and brain regions with significant WMV/CSFV changes were yielded based on a voxel-level height threshold of $P < 0.005$, Family Wise Error (FWE) corrected..

DTI preprocessing and voxel-based analysis (VBA)

First of all, the fractional anisotropy (FA) of each rat was calculated in FSL [11]. The preprocessing and data analysis were performed using the SPM12 (Welcome Department of Cognitive Neurology, London, UK). The volume of which $b = 0$ of each participant's original image was spatially normalized to the EPI-template in Paxinos & Watson space and carried the FA images along [12]. Then, all the normalized FA images were resliced by $1.0 \times 1.0 \times 1.5\ mm^3$ voxels (after zooming) and smoothed by a Gaussian kernel of 3 mm full width at half-maximum (FWHM). ROIs were selected from the Paxinos & Watson space and save as mask images, and the mean FA, ADC and voxels of these ROIs were extracted. Furthermore, preprocessed FA and ADC images were analyzed within SPM12 based on the framework of the general linear model. Two-sample *t*-tests were performed in SPM12. Cerebellar regions with significant FA and ADC changes in rats were yielded based on a voxel-level height threshold of $P < 0.005$ (FWE corrected).

Brain structural network

This study follows the general method to analyze the topological properties of brain networks based on the structural connectivity between brain regions: bilateral bulbar medulla, pons, red nucleus, flocculonodular lobe, anterior cerebellar lobe, posterior cerebellar lobe, cerebellar nucleus, lateral thalamic nucleus. The FA value of the bundles between t brain regions extracted via white matter fiber template in the Paxinos & Watson space and regarded as the structural connections. Rat brain structural network were constructed via BrainNet Viewer and topological properties were calculated as described previously [13].

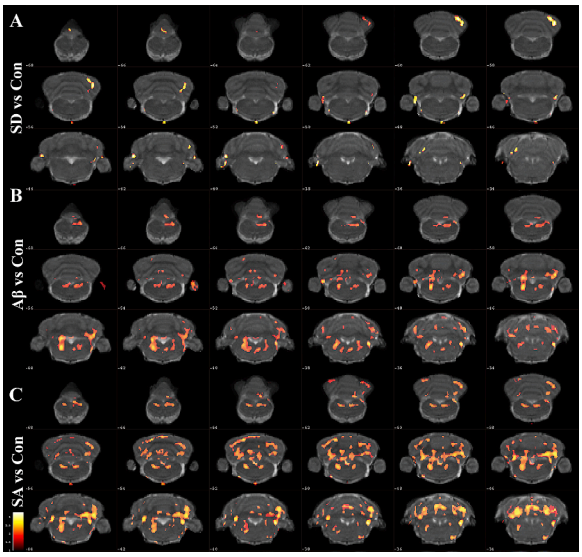

Fig. 1. Statistical parametric maps of FA in cerebellum with voxel-wise analysis. Regional difference of FA value between Con and SD (A), Aβ (B), SA (C) groups were compared, and specific significant clusters were showed in Table 1-3.

Statistical analysis

All statistical analyses were carried out by R package and data are expressed as means ± standard deviation (SD). To be more specific, one-way analysis of variance (ANOVA) with Turkey's multiple comparisons test was used for within-group comparisons and independent sample paired *t*-test was performed for bilateral hemisphere comparisons via R package (ggplot2, version 3.6.3). Data distribution was tested for normality with Shapiro-Wilk test. If the data were not normally distributed, nonparametric Kruskal-Wallis tests were used; if the equal variances not assumed, Games-Howell tests were applied.

Results

Sleep deprivation combined with AβO led to an increased FA value in the anterior lobe of cerebellum

The cerebellum is classically divided into the anterior lobe, the posterior lobe, and the flocculonodular lobe, responsible for the sensorimotor connections, cognition and equilibrium respectively [14,15]. Fractional anisotropy (FA), although proved to be useful in the characterization of microstructural damage of white matter [16], has also been demonstrated to be as a proxy of the cerebellum cortex integrity [17]. In order to assess the changes of FA value in the cerebellum, we first made statistical parametric maps of FA in cerebellum with voxel-wise analysis (Fig. 1). Regional difference of FA value between Con and SD, Aβ, SA groups were compared and significant different clusters were showed in Tables 1–3. Our results showed that, compared to the Con group, there are only a few different pixel clusters in the SD group. While in the Aβ group, there are more pixel clusters with significant differences. In the SA group, the significant different pixel clusters further expand.

Furthermore, we assessed the average FA values in the three cerebellar lobes. As shown in Fig. 2, compared to Con or SD group, there was a significant increased FA value in SA group in either side of the anterior lobe (Left side, $P = 0.0051$ vs Con, $P = 0.0006$ vs SD; Right side, $P < 0.0001$ vs Con; $P < 0.0001$ vs SD; $P = 0.007$ vs Aβ) (Fig. 2A-C). Whereas in both side of the posterior lobe, there was a significant decreased FA values only in Aβ group (Left side, $P = 0.0289$ vs Con; Right side, $P = 0.0141$ vs Con; $P = 0.0013$ vs SD group) (Fig. 2D-F), but no significant changes of FA in the flocculonodular lobe (data not shown). These results suggest, although sleep deprivation alone has limited impact, their combined effect of sleep deprivation and AβO can lead to a significant damage to cerebellar anterior lobe.

Sleep deprivation combined with AβO led to decreased ADC value in the cerebellar lobes and cerebellar nuclei

The apparent diffusion coefficient (ADC) is a parameter that describes the diffusion ability of water molecules. The faster the diffusion, the larger the ADC value. ADC is sensitive to changes in the biological environment and could reflect the integrity of cell membranes. For example, some acute neuropathological conditions involved in cellular edema present reduced ADC value; while neurodegeneration might result in an increased diffusion of water molecule, then an increased ADC value accordingly [18]. To investigate the effects of sleep deprivation and AβO on the diffusion ability of water molecules in the cerebellum, we evaluated the ADC values in the three cerebellar lobes and the cerebellar nuclei.

We first made statistical parametric maps of ADC in cerebellum with voxel-wise analysis (Fig. 3). Regional difference of ADC value between Con and other three groups were compared and specific significant different clusters were showed in Tables 4–6. Next we further assessed the average ADC value of the cerebellum. Our results showed that there was a significant decreased ADC value on both sides of the anterior lobe in the SA group (Left side, $P = 0.0045$ vs Con, $P = 0.012$ vs SD, $P = 0.0349$ vs Aβ; Right side, $P = 0.0002$ vs Con, $P < 0.0001$ vs SD) (Fig. 4A-C). Besides that, a decreased ADC value on the right side of anterior lobe was also observed in the Aβ group ($P = 0.0288$ vs Con) (Fig. 4B).

In bilateral cerebellar posterior lobes, the decreased ADC values were observed in both Aβ group and SA group (Aβ group: left side, $P = 0.0244$ vs Con; right side, $P = 0.0012$ vs Con; SA group: left side, $P = 0.0003$ vs Con; right side, $P = 0.002$ vs Con) (Fig. 4D-F). In SD group, there was only a significant decreased ADC value in the left side ($P = 0.0052$ vs Con) (Fig. 4D,E). No significant ADC value changes were found in the flocculonodular lobe (data not shown).

Table 1
Clusters revealed difference of FA in the cerebellum between Con and SD groups with Family Wise Error (FWE) corrected.

Region	Voxels	T Value	X	Y	Z
cerebellum_anterior lobe of cerebellum_left	31	3.788	3.7788	4.2315	−13.3179
cerebellum_cerebellar nucleus_right	1	2.8595	3.7788	5.2581	−13.3179
cerebellum_posterior lobe of cerebellum_left	21	3.462	3.7788	3.789	−13.3179
cerebellum_posterior lobe of cerebellum_right	286	3.702	3.7854	3.2475	−13.7979
cerebellum_anterior lobe of cerebellum_left	56	3.2394	−2.8134	3.8136	−9.4779
pfi flocculonodular lobe_left	74	3.9269	−5.2288	6.0526	−9.9579
pfi flocculonodular lobe_left	50	3.4588	−4.3893	6.4116	−11.8779
pfi flocculonodular lobe_right	19	3.5415	4.0292	6.1303	−11.3979
pfi flocculonodular lobe_right	31	3.6091	5.3547	6.0054	−10.9179
pfi flocculonodular lobe_left	73	3.7082	−5.2156	4.9696	−10.9179

Notice: FA value changes were yielded based on a voxel-level height threshold of $P < 0.005$ and a cluster-extent threshold of 20 voxels.

Table 2
Clusters revealed difference of FA in the cerebellum between Con and Aβ groups with FWE corrected.

Region	Voxels	T Value	X	Y	Z
cerebellum_anterior lobe of cerebellum_left	153	3.3918	−1.5867	5.6886	−11.8779
cerebellum_anterior lobe of cerebellum_right	74	3.8246	−1.5933	5.5044	−11.3979
cerebellum_cerebellar nucleus_left	224	4.0116	−1.5999	5.7627	−10.9179
cerebellum_cerebellar nucleus_right	7	3.0587	−1.5999	6.0459	−10.9179
cerebellum_posterior lobe of cerebellum_left	195	3.4307	−1.5867	5.6886	−11.8779
cerebellum_posterior lobe of cerebellum_right	283	3.4829	−1.5405	6.5709	−15.2379
cerebellum_anterior lobe of cerebellum_left	431	3.7476	2.9302	5.1545	−9.4779
cerebellum_anterior lobe of cerebellum_right	738	4.4831	2.9368	6.8078	−9.9579
cerebellum_cerebellar nucleus_left	14	3.0506	2.95	5.5832	−10.9179
cerebellum_cerebellar nucleus_right	149	3.773	2.9566	5.7674	−11.3979
cerebellum_posterior lobe of cerebellum_left	137	3.4425	2.9368	3.8873	−9.9579
cerebellum_posterior lobe of cerebellum_right	468	4.2439	2.9566	5.1833	−11.3979
pfi flocculonodular lobe_right	14	3.2261	2.95	5.4416	−10.9179
pfi flocculonodular lobe_left	83	4.4704	−4.2443	6.3206	−12.3579

Notice: FA value changes were yielded based on a voxel-level height threshold of $P < 0.005$ and a cluster-extent threshold of 20 voxels.

Table 3
Clusters revealed difference of FA in the cerebellum between Con and SA groups with FWE corrected.

Region	Voxels	T Value	X	Y	Z
cerebellum_anterior lobe of cerebellum_left	1539	4.5939	−1.0834	4.1968	−9.4779
cerebellum_anterior lobe of cerebellum_right	2027	4.9531	−1.0702	6.3352	−10.4379
cerebellum_cerebellar nucleus_left	386	4.3631	−1.0636	5.6344	−10.9179
cerebellum_cerebellar nucleus_right	375	4.1085	−1.0636	6.0769	−10.9179
cerebellum_posterior lobe of cerebellum_left	1308	4.0943	−1.0438	2.2576	−12.3579
cerebellum_posterior lobe of cerebellum_right	1854	4.5052	−1.057	4.9513	−11.3979
pfi flocculonodular lobe_left	132	3.2914	−1.0438	5.6206	−12.3579
pfi flocculonodular lobe_right	49	3.8117	−1.0636	5.2096	−10.9179
pfi flocculonodular lobe_left	41	3.3971	−5.3433	6.2298	−10.4379
pfi flocculonodular lobe_right	2	2.9851	2.8512	6.2733	−13.7979
pfi flocculonodular lobe_left	26	3.2764	−4.5343	5.3344	−11.3979
pfi flocculonodular lobe_left	50	3.0865	−5.0838	4.7757	−10.4379

Notice: FA value changes were yielded based on a voxel-level height threshold of $P < 0.005$ and a cluster-extent threshold of 20 voxels.

In the left side cerebellar nuclei, there was a significant decreased ADC value in Aβ group and SA group (Aβ group, P = 0.0084 vs Con; SA group, P = 0.0016 vs Con) (Fig. 4G,H). What's more, the significant difference of ADC values were found between left and right sides of the cerebellar nuclei in both SD and SA groups (SD group: P = 0.0005; SA group: P = 0.0422) (Fig. 4I).

Sleep deprivation combined with AβO increased the volume of cerebellum

VBM analysis is a morphological method to detect regions where gray matter and white matter concentration differs significantly between groups. It is not biased to one specific structure and could provide a comprehensive and impartial assessment of structural differences throughout the brain [19]. Using VBM analysis, Colloby *et al.* found cerebellar gray matter loss in AD patients [20]. To reveal the changes of cerebellum volume under our experimental condition of sleep deprivation combined with AβO, using voxel-wise analysis, we first made statistical parametric maps of volume in cerebellum (Fig. 5), the significant different clusters of volume between Con and SD, Aβ, SA groups were showed in Tables 7–9. Next, we further compared the mean volume of three cerebellar lobes. As shown in Fig. 6, we found, compared to Con group, SA group showed significant increased volumes in the left side of anterior lobe (P = 0.0005 vs Con), bilateral posterior lobes (P = 0.0387 vs Con for the left side, P = 0.0123 vs Con for the right side) and right side of flocculonodular lobe (P = 0.0341 vs Con), while there was no statistical difference in SD or Aβ groups. These results suggest that sleep deprivation or AβO alone had little effect on cerebellar volume, but their coaction led to an increased cerebellar volume.

Sleep deprivation exacerbated the detrimental effect of AβO on the cerebellar structural network

The structural network of brain is derived from diffusion-MRI and models the white matter tracts that transfer information between spatially isolated gray-matter areas. Structural network connectivity could be mapped in vivo with tractography [21,22]. The changes of structural connectivity can be used to predict the degradation of white matter fiber bundles and the strength of functional brain networks [23]. Some alterations of the structural connectivity have been reported in MCI or AD patients, which indicated that the altered structural network properties maybe present at very early stages when the AD-related pathological landmarks are not yet obvious [24–26]. However, the cerebellar structural connectivity is often overlooked in research on AD or sleep disorders. In order to explore the impact of sleep deprivation and AβO on the cerebellar network, we mapped the cerebellar structural network based on the

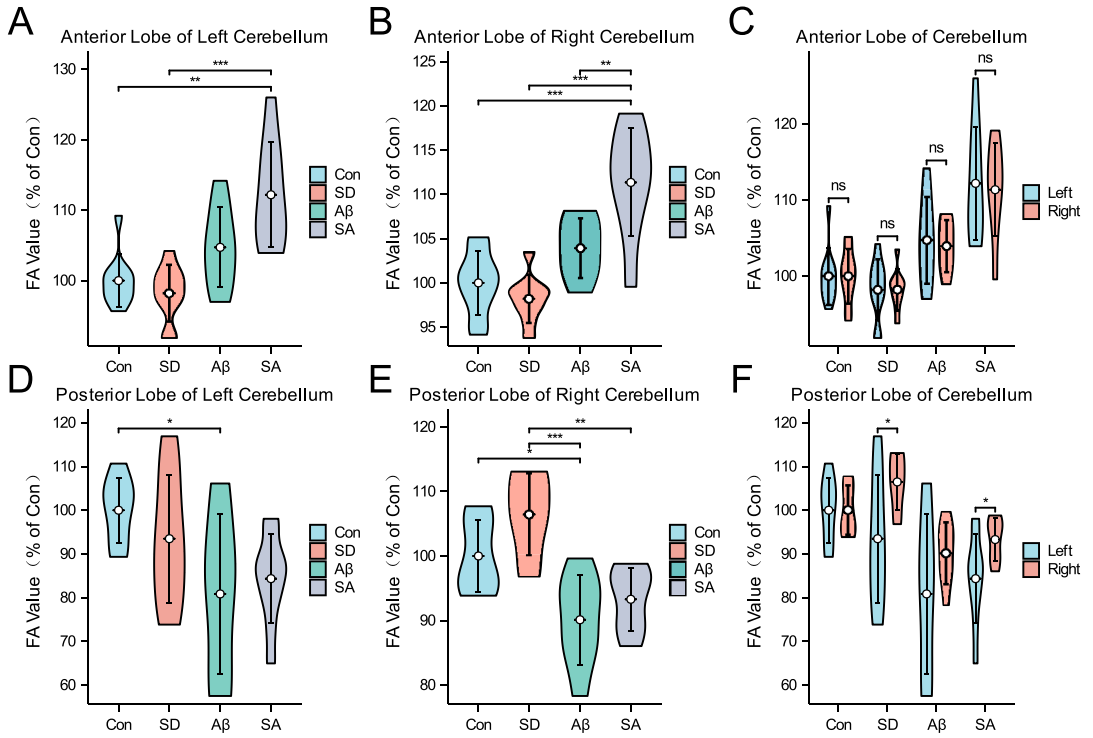

Fig. 2. Sleep deprivation combined with AβO led to an increase of FA value in the anterior lobe of cerebellum. Quantification of the mean FA value in left and right side of anterior lobe (A, B) and posterior lobe (D, E), and between left and right anterior (C) and posterior lobes (F). $*p < 0.05$, $**p < 0.01$, $***p < 0.001$. n = 7–11 rats/group.

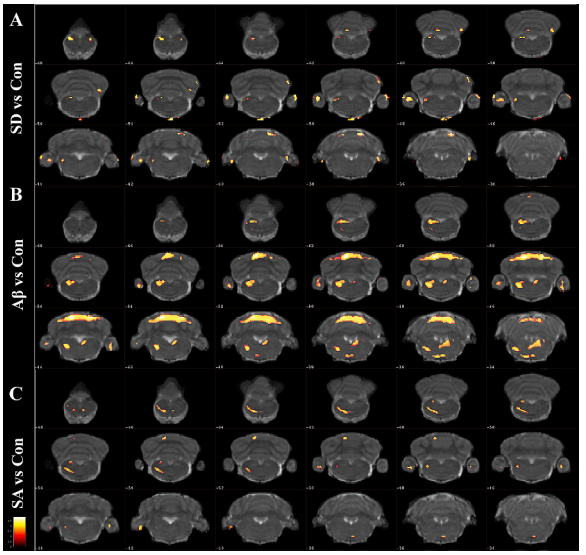

Fig. 3. Statistical parametric maps of ADC in cerebellum with voxel-wise analysis. Regional difference of ADC value between Con and SD (A), Aβ (B), SA (C) groups were compared, and specific significant clusters were showed in Table 4-6.

nodes and tracts between the cerebellum (three lobes and cerebellar nuclei) and the thalamus (lateral nucleus), the brain stem (medulla, pons and red nucleus) (Fig. 7A and Table 10). Our results showed that, compared to Con group, a significant enhanced connection strength was observed in the pontine transverse fibers and the right superior cerebellar peduncle in Aβ group. In SA group, the strengthened connectivity was further extended to bilateral superior cerebellar peduncles. There was no significant strength change in the internodal connection in SD group. These results suggest that the cerebellar structural network may be more susceptible

Table 4
Clusters revealed difference of ADC in the cerebellum between Con and SD groups with FWE corrected.

Region	Voxels	T Value	X	Y	Z
cerebellum_anterior lobe of cerebellum_right	2	2.8852	6.1637	7.1632	−11.8779
cerebellum_anterior lobe of cerebellum_left	17	3.4474	−5.8598	6.3266	−11.8779
cerebellum_anterior lobe of cerebellum_right	5	3.0787	−5.8664	6.4256	−11.3979
cerebellum_anterior lobe of cerebellum_left	2	2.8765	−1.4681	6.8963	−10.4379
cerebellum_posterior lobe of cerebellum_left	17	3.0652	−1.4087	6.8372	−14.7579
cerebellum_anterior lobe of cerebellum_right	116	3.586	2.0026	1.9394	−9.9579
cerebellum_posterior lobe of cerebellum_right	18	3.5024	2.0092	1.982	−10.4379
pfi flocculonodular lobe_right	92	3.3106	6.1637	6.4375	−11.8779
pfi flocculonodular lobe_left	170	3.3978	−5.8598	6.4682	−11.8779
pfi flocculonodular lobe_right	77	3.2499	4.8052	6.9158	−9.9579
pfi flocculonodular lobe_left	67	3.2254	−6.6754	5.7103	−10.4379

Notice: ADC value changes were yielded based on a voxel-level height threshold of $P < 0.005$ and a cluster-extent threshold of 20 voxels.

Table 5
Clusters revealed difference of ADC in the cerebellum between Con and Aβ groups with FWE corrected.

Region	Voxels	T Value	X	Y	Z
cerebellum_anterior lobe of cerebellum_right	64	3.483	−0.6789	6.4572	−9.9579
cerebellum_posterior lobe of cerebellum_right	11	3.1711	−0.6525	6.6276	−11.8779
cerebellum_posterior lobe of cerebellum_left	79	3.3277	−1.9714	6.7774	−12.8379
cerebellum_anterior lobe of cerebellum_left	13	3.1866	−5.3235	6.3576	−11.8779
cerebellum_anterior lobe of cerebellum_right	2	2.9144	−5.3301	6.4566	−11.3979
cerebellum_anterior lobe of cerebellum_left	1178	4.8238	−0.9186	2.0388	−11.3979
cerebellum_anterior lobe of cerebellum_right	1222	4.6134	−0.9252	1.8546	−10.9179
cerebellum_cerebellar nucleus_right	1	2.8835	−0.8922	2.6517	−13.3179
cerebellum_posterior lobe of cerebellum_left	784	4.9471	−0.912	1.9398	−11.8779
cerebellum_posterior lobe of cerebellum_right	676	4.7653	−0.9252	1.8546	−10.9179
pfi flocculonodular lobe_right	32	3.0984	5.489	6.3985	−11.8779
pfi flocculonodular lobe_left	93	3.2395	−5.3301	6.7575	−11.3979

Notice: ADC value changes were yielded based on a voxel-level height threshold of $P < 0.005$ and a cluster-extent threshold of 20 voxels.

Table 6
Clusters revealed difference of ADC in the cerebellum between Con and SA groups with FWE corrected.

Region	Voxels	T Value	X	Y	Z
pfi flocculonodular lobe_left	23	3.7267	−5.3433	7.0971	−10.4379
pfi flocculonodular lobe_left	16	3.1812	−5.7214	7.2019	−11.8779
pfi flocculonodular lobe_right	9	2.9262	5.2163	7.4665	−10.9179
cerebellum_posterior lobe of cerebellum_left	16	3.0391	−1.7119	6.5092	−12.8379
cerebellum_anterior lobe of cerebellum_left	8	3.0007	−1.0504	2.215	−11.8779
cerebellum_posterior lobe of cerebellum_left	83	3.4061	−1.0438	1.9744	−12.3579

Notice: ADC value changes were yielded based on a voxel-level height threshold of $P < 0.005$ and a cluster-extent threshold of 20 voxels.

to AβO than to sleep deprivation. Short-term fragmented sleep deprivation may not lead to significant abnormalities in the cerebellar structural connectivity, but sleep deprivation might exacerbate the damage of AβO to the cerebellar structural connectivity.

Furthermore, we assessed the related topological properties of rich-club, shortest path length (Lp), and small world network (SMN). Except a significant reduced rich-club was revealed in Aβ group, no any other changes of topological properties were found in SD or SA group (Fig. 7B-E).

Discussion

Cerebellum has often been dismissed in MRI studies of AD and sleep disorders. In our present study, we found sleep deprivation combined with AβO led to alterations of FA, ADC, volume of cerebellum and abnormal structural network connectivity. Our results suggest that the cerebellum is involved in the early progression of AD, and AβO-induced pathological damage to cerebellum may be further exacerbated by sleep disorders.

By assessment of FA values in the cerebellum, we found increased FA in the cerebellar anterior lobes in SA group, which might indicate the disruption of cerebellum cortex integrity and gliosis [27,28] induced by sleep deprivation and AβO neurotoxicity, since either of them could activate the astrocyte [29,30]. In addition, the increased FA might suggest a hyperconnectivity, which leads to the imbalance in the circuits related with cerebral cognition [31,32]. Meanwhile, in SA group, we also found the strengthened connectivity in both sides of the superior cerebellar peduncles, the increased FA causing the injury integrity of the cerebellum also may be related

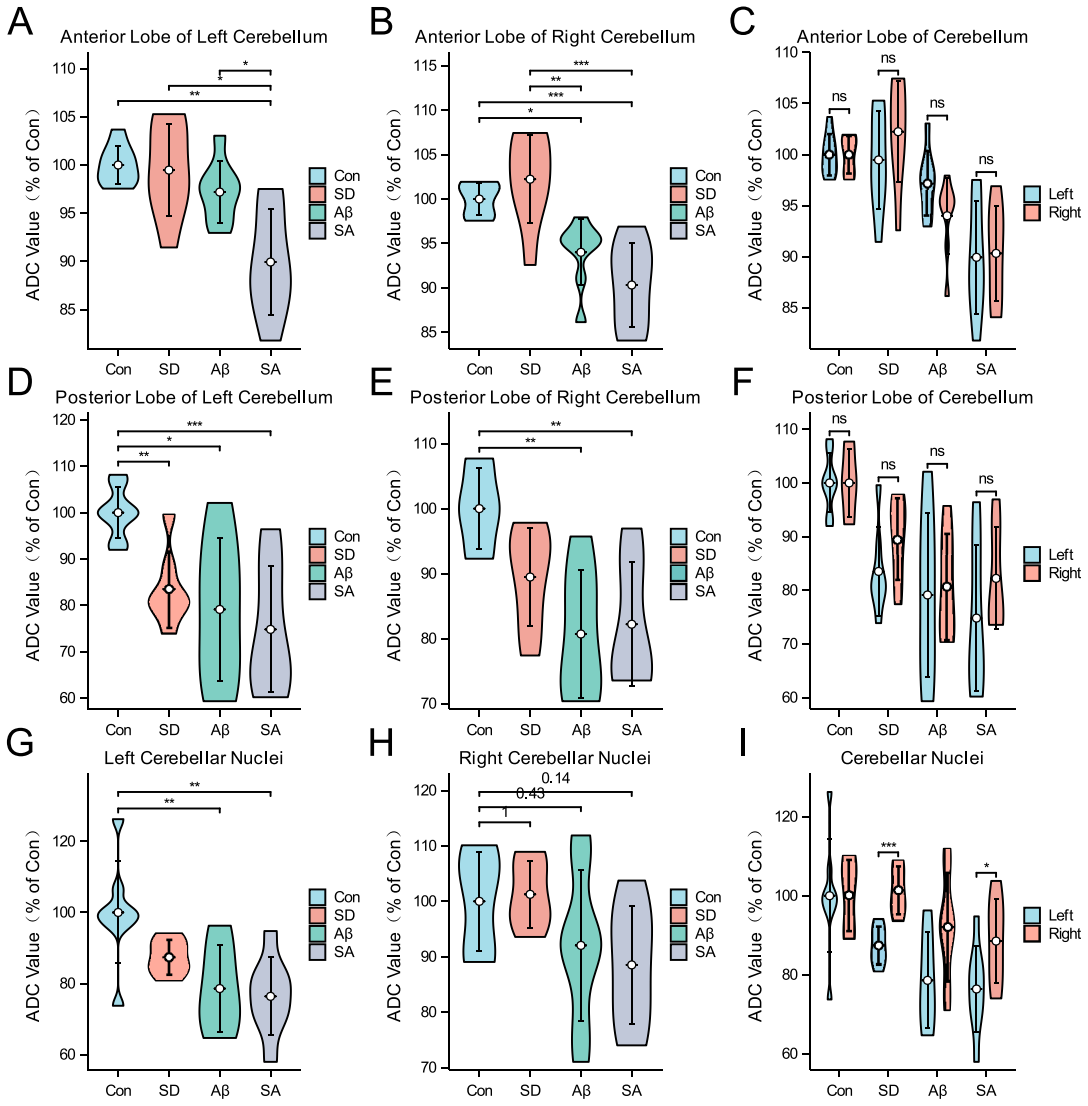

Fig. 4. Sleep deprivation combined with AβO led to decreased ADC values in the cerebellar lobes and cerebellar nuclei. Quantification of the mean ADC value in left and right side of anterior lobe (A, B), posterior lobe (D, E), cerebellar nuclei (G, H) and bilateral differences (C, F, I). $*p < 0.05$, $**p < 0.01$, $***p < 0.001$. n = 7–10 rats/group.

with the abnormal brain network [17].

Many studies have demonstrated that adequate sleep could promote free water diffusivity and thereby induce increased ADC value [18,33,34]. Based on these, our finding that decreased ADC values in SA group is most possibly associated with restricted free water diffusivity caused by sleep deprivation.

The cerebellum is involved in a wide range of non-motor function, including sensorimotor modulation, visual spatial processing, executive function as well as linguistic skills. The anatomical basis of these proposed functions is the existence of cerebro-cerebellar circuits, mainly composed of cortico-ponto-cerebellar and cerebello-thalamo-cortical loops, which link the cerebellum with motor cortices, association cortices and paralimbic regions [35,36]. In our present study, we found an enhanced connectivity in the pontine transverse fibers and the right superior cerebellar peduncle in Aβ group, which might indicate a compensatory response of the cerebellum at early stages of disease [37]. This change also implied that the right cerebellar nuclei and right superior cerebellar peduncle are more sensitive to AβO neurotoxicity [38]. The current finding is consistent with the notion that AD is a dysfunction of brain network [39,40]. This increased connection in the right superior cerebellar peduncle may reflect deregulated neural activation or partly network-breakdown resulting from AβO-induced hyperexcitability [41]. Meanwhile the strengthened connectivity was expanded to bilateral superior cerebellar peduncles under condition of sleep deprivation combined with AβO, indicating more severer damage and network disruption. We also found the rats in SA group showed significant cognitive decline (data not shown), which is very likely associated with the abnormal cerebellar structural connection, since the cerebellar network could regulate the cognitive

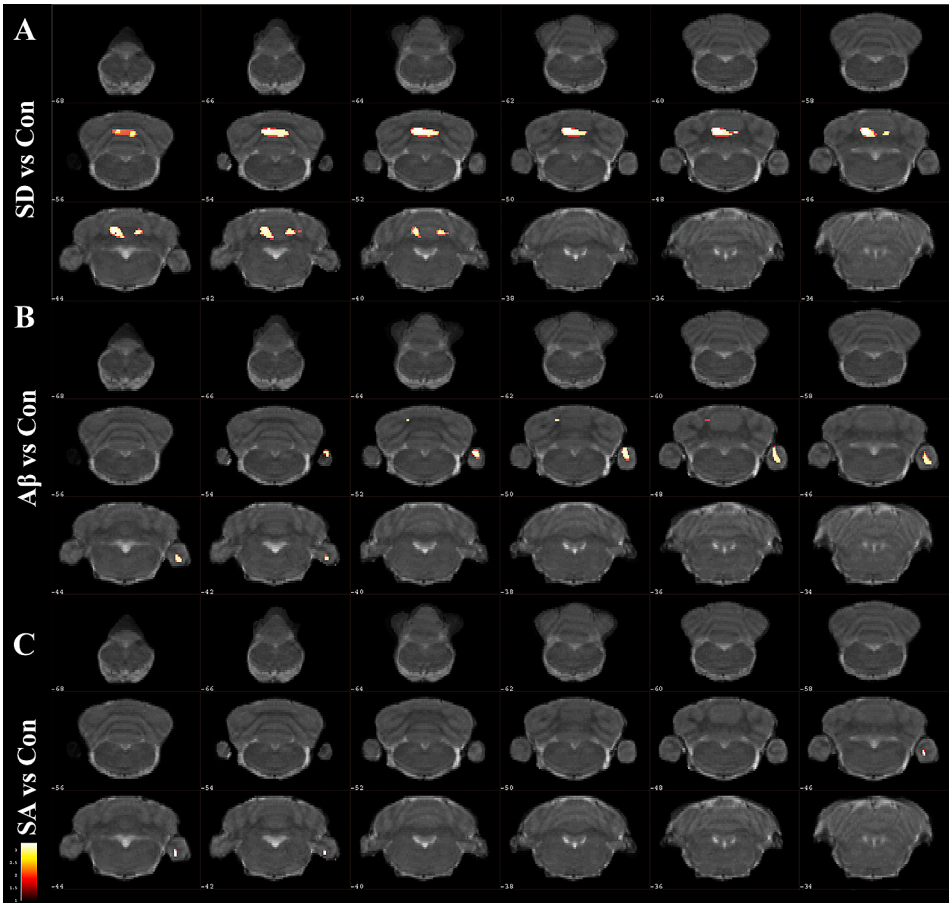

Fig. 5. Statistical parametric maps of volume in cerebellum with voxel-wise analysis. Regional difference of volume between Con and SD (A), Aβ (B), SA (C) groups were compared, and specific significant clusters were showed in Table 7-9.

Table 7
Clusters revealed difference of volume in the cerebellum between Con and SD groups with FWE corrected.

Region	Voxels	T Value	X	Y	Z
cerebellum_anterior lobe of cerebellum_left	415	3.2576	−0.7843	3.4408	−12.3579
cerebellum_anterior lobe of cerebellum_right	160	3.0034	−0.8041	3.6139	−10.9179
cerebellum_cerebellar nucleus_left	1	2.8761	−0.7777	3.7843	−12.8379
cerebellum_posterior lobe of cerebellum_left	335	3.2769	−0.7843	3.4408	−12.3579
cerebellum_posterior lobe of cerebellum_right	255	3.0881	−0.7843	3.6001	−12.3579

Notice: Volume changes were yielded based on a voxel-level height threshold of $P < 0.005$ and a cluster-extent threshold of 20 voxels.

Table 8
Clusters revealed difference of volume in the cerebellum between Con and Aβ groups with FWE corrected.

Region	Voxels	T Value	X	Y	Z
cerebellum_anterior lobe of cerebellum_right	11	2.9985	5.3679	6.6747	−11.8779
pfi flocculonodular lobe_right	64	2.9881	5.3679	6.5331	−11.8779
cerebellum_anterior lobe of cerebellum_left	8	2.9029	−1.8396	2.7957	−12.3579
cerebellum_posterior lobe of cerebellum_left	18	2.9065	−1.8396	2.7957	−12.3579

Notice: Volume changes were yielded based on a voxel-level height threshold of $P < 0.005$ and a cluster-extent threshold of 20 voxels.

function in early AD [42]. In addition, it has been demonstrated that the cerebellum may play critical roles in sleep regulation [43,44]. A study on cats showed that the lesions of the superior cerebellar peduncle caused a decreased NREM and REM sleep [45]. The cerebellar output, mainly through the superior cerebellar peduncle, could modulate thalamo-cortical spindles [46], thereby

Table 9
Clusters revealed difference of volume in the cerebellum between Con and SA groups with FWE corrected.

Region	Voxels	T Value	X	Y	Z
pfi flocculonodular lobe_right	3	2.9381	5.2163	7.4665	−10.9179

Notice: Volume changes were yielded based on a voxel-level height threshold of $P < 0.005$ and a cluster-extent threshold of 20 voxels.

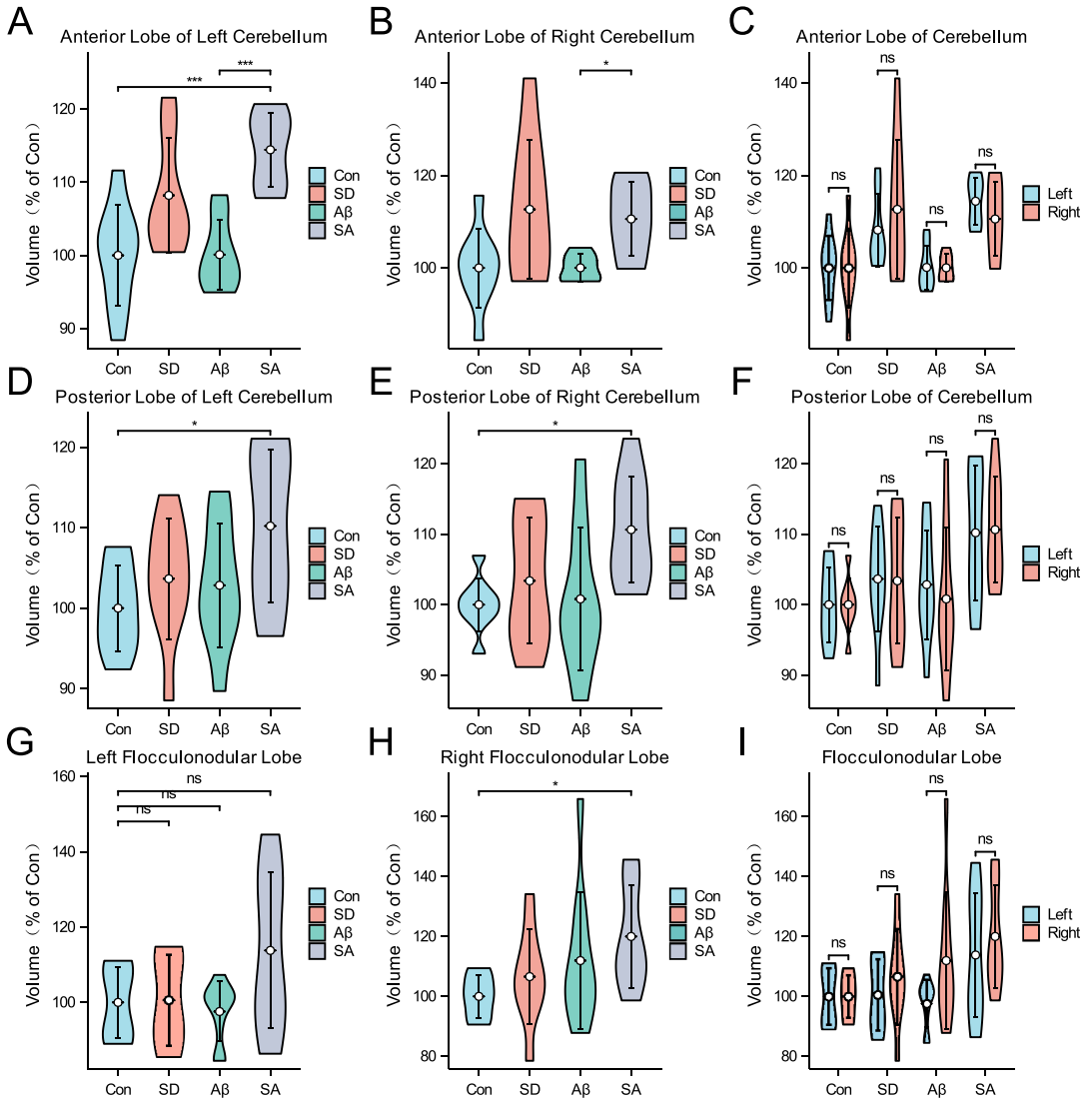

Fig. 6. Sleep deprivation combined with AβO increased the volume of cerebellum. Quantification of the volume in left and right side of anterior (A, B), posterior lobe (D, E), flocculonodular lobe (G, H) and bilateral differences (C, F, I). *$p < 0.05$, ***$p < 0.001$. n = 6–10 rats/group.

influencing neocortical learning and cognitive processes during sleep. Therefore, although no significant changes of structural cerebellar network was detected in our experimental condition of short sleep deprivation, we have reason to infer that chronic or long term sleep deprivation could disturb cerebellar activity and thereby further aggravate AβO-induced cognitive impairment through affecting cortico-ponto-cerebellar-thalamo-cortical circuit [47]. This abnormal cerebellar network connectivity caused by sleep disorder is very likely to be linked with the increased risk of AD.

Recently, Um YH *et al.* demonstrated changes of cerebellar volume is associated with increased odds of the disease progression [48]. In the present work, we observed the increased volume in most regions of cerebellum, including both sides of the posterior lobe, the left anterior lobe and right flocculonodular lobe in SA group. This finding, inconsistent with the reports of decreased cerebellar volume in AD from many literatures [49,50], might indicate an early compensatory response. In addition, the larger cerebellar volume might be related with worse cognitive outcome [42]. A cohort study in MCI and AD patients revealed cerebellum volume is negatively associated

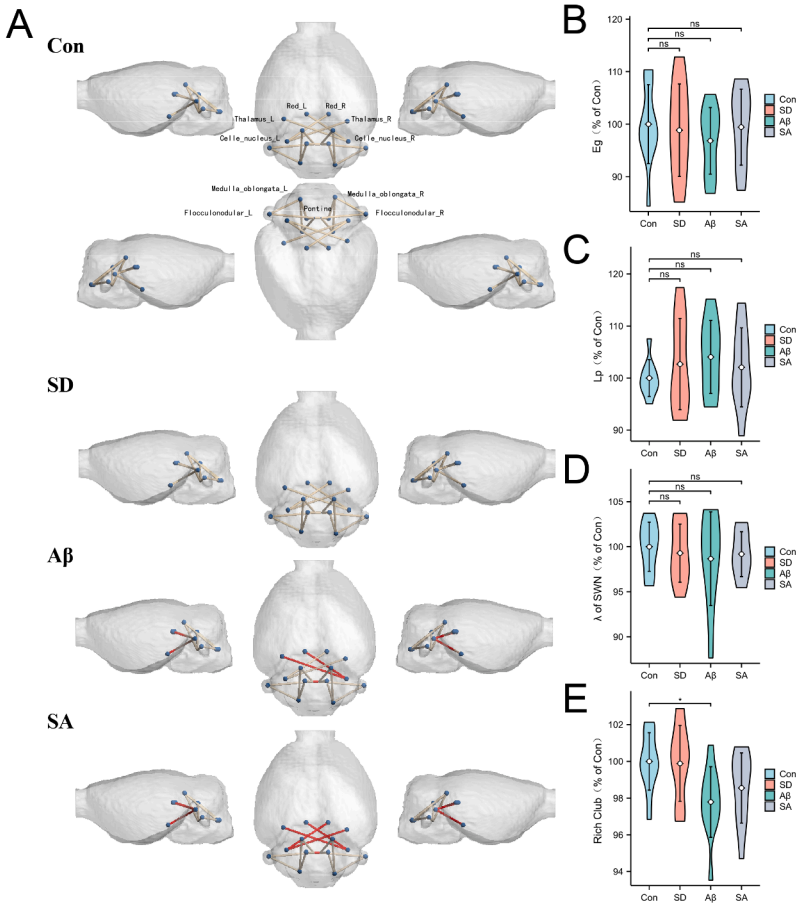

Fig. 7. Sleep deprivation exacerbated the detrimental effect of AβO on the cerebellar structural network. (A) A graph of brain structural network in Con group (ROIs were labelled near the nodes. Red, red nucleus; Celle_nucleus, cerebellar nucleus; L, left; R, right) and the alterations of the structural network connectivity in SD group (SD), Aβ group (Aβ) and SA group (SA) respectively. The strenthened connectivity was presented as red edge, n = 6–11 rats/group. Source data are provided in Table 10. (B-E) Quantification of the global efficiency (Eg) (B), length of shortest path (Lp) (C), the σ property of small world network (SWN) (D) and rich club (E). *$p < 0.05$, n = 9–11 rats/group. (For interpretation of the references to colour in this figure legend, the reader is referred to the web version of this article.)

with the cognitive function in MCI patients, the increased cerebellar volume could be considered as a potential marker for predicting early cognitive decline [34]. Another recent study verified an overall higher cerebellar prediction accuracy than the whole brain, presenting with higher anterior cerebellar contribution to MCI and higher posterior cerebellar contribution to mild to moderate AD [51]. Our findings further confirmed the cerebellum is involved in early AD. The more detailed underlying mechanism need to investigate in future. Additionally, we found no significant changes of cerebellum volume under conditions of sleep deprivation alone, this is contrary to a decreased volume in the anterior lobes of the cerebellum and cerebellar nuclei found in patients with REM sleep disturbances [52]. One reason for this inconsistence may be due to the relatively shorter time of sleep deprivation in our study.

In conclusion, from the structural MRI changes of cerebellum, we provide important experimental evidence to prove that sleep deprivation could exacerbate the damage to the cerebellum induced by AβO, which may be one reason for sleep disorder increasing the risk of AD. Our data would contribute to recognizing the enigmatic role of cerebellum in AD and sleep loss, and aid in the development of non-invasive MRI biomarker in the cerebellum for the screening and diagnosis early-stage AD, especially in individuals with self-reported sleep disorders.

Funding

This study was supported by grants from the Scientific Research Key Program of Beijing Municipal Commission of Education (KZ202110025032), the National Natural Science Foundation of China (81771370, 82071514), the National Key Research and Development Program of China (2020YFC2005300, 2022YFC2503900) and the Scientific Research Common Program of Beijing Municipal Commission of Education (KM201810025004, KM202110025029).

Table 10
Structural connection in matrix revealed a difference between groups.

Region in Matrix Left, row of matrix; Right, column of matrix.		Mean r Value (% of Con) in Four Groups				One-way ANOVA with Turkey's Post-hoc, vs Con (P Value)		
		Con	SD	Aβ	SA	SD	Aβ	SA
Medulla_L	Flocculonodular lobe_L	100.0 ± 13.70	100.0 ± 37.20	102.4 ± 42.48	120.7 ± 44.53	>0.9999	0.9987	0.5527
Medulla_L	Anterior lobe_L	100.0 ± 13.70	100.0 ± 37.20	102.4 ± 42.48	120.7 ± 44.53	>0.9999	0.9987	0.5527
Medulla_L	Posterior lobe _L	100.0 ± 13.70	100.0 ± 37.20	102.4 ± 42.48	120.7 ± 44.53	>0.9999	0.9987	0.5527
Pons_L	Flocculonodular lobe_L	100.0 ± 4.49	99.5 ± 4.18	99.6 ± 4.43	110.7 ± 5.92	0.9955	0.9978	0.0006*
Pons_L	Anterior lobe_L	100.0 ± 4.49	99.5 ± 4.18	99.6 ± 4.43	110.7 ± 5.92	0.9955	0.9978	0.0006*
Pons_L	Posterior lobe _L	100.0 ± 4.49	99.5 ± 4.18	99.6 ± 4.43	110.7 ± 5.92	0.9955	0.9978	0.0006*
Cerebellar nucleus_L	Red nucleus_R	100.0 ± 3.62	96.3 ± 3.86	105.6 ± 7.52	108.1 ± 6.99	0.4175	0.1356	0.0142*
Cerebellar nucleus_L	Tha_lateral nucleus_R	100.0 ± 3.62	96.3 ± 3.86	105.6 ± 7.52	108.1 ± 6.99	0.4175	0.1356	0.0142*
Pons_L	Pons_R	100.0 ± 4.74	102.0 ± 12.09	119.2 ± 18.15	117.9 ± 11.88	0.9865	0.0118	0.0329*
Cerebellar nucleus_R	Red nucleus_L	100.0 ± 3.46	95.9 ± 4.25	107.0 ± 8.01	108.1 ± 6.10	0.4369	0.0395	0.0137*
Cerebellar nucleus_R	Tha_lateral nucleus_L	100.0 ± 3.46	95.9 ± 4.25	107.0 ± 8.01	108.1 ± 6.10	0.4369	0.0395	0.0137*
Medulla_R	Flocculonodular lobe_R	100.0 ± 7.07	93.9 ± 40.09	88.8 ± 34.06	108.9 ± 49.52	0.9793	0.8865	0.9390
Medulla_R	Anterior lobe_R	100.0 ± 7.07	93.9 ± 40.09	88.8 ± 34.06	108.9 ± 49.52	0.9793	0.8865	0.9390
Medulla_R	Posterior lobe _R	100.0 ± 7.07	93.9 ± 40.09	88.8 ± 34.06	108.9 ± 49.52	0.9793	0.8865	0.9390
Pons_R	Flocculonodular lobe_R	100.0 ± 7.11	103.0 ± 4.01	109.2 ± 10.43	111.4 ± 11.76	0.8937	0.1759	0.0364*
Pons_R	Anterior lobe_R	100.0 ± 7.11	103.0 ± 4.01	109.2 ± 10.43	111.4 ± 11.76	0.8937	0.1759	0.0364*
Pons_R	Posterior lobe _R	100.0 ± 7.11	103.0 ± 4.01	109.2 ± 10.43	111.4 ± 11.76	0.8937	0.1759	0.0364*

Note: r values were represented as mean ± standard deviations. *p means statistic difference ($P < 0.05$).
Abbreviations: L, Left, R, Right, Con, Control Group, SD, Sleep Deprivation Group, Aβ, β-amyloid Injection Group, SA Sleep Deprivation with β-amyloid Injection Group, Tha, thalamus.

Declaration of Competing Interest

The authors declare that they have no known competing financial interests or personal relationships that could have appeared to influence the work reported in this paper.

References

[1] Panza F, Lozupone M, Logroscino G, Imbimbo BP. A critical appraisal of amyloid-β-targeting therapies for Alzheimer disease. Nat Rev Neurol 2019;15:73–88.
[2] Yu H, Wang M, Yang Q, Xu X, Zhang R, Chen Xi, et al. The electrophysiological and neuropathological profiles of cerebellum in APPswe/PS1ΔE9 mice: a hypothesis on the role of cerebellum in Alzheimer's disease. Alzheimers Dement 2023;19(6):2365–75.
[3] Mann DMA, Jones D, Prinja D, Purkiss MS. The prevalence of amyloid (A4) protein deposits within the cerebral and cerebellar cortex in Down's syndrome and Alzheimer's disease. Acta Neuropathol 1990;80(3):318–27.
[4] Bruchhage MMK, Correia S, Malloy P, Salloway S, Deoni S. Machine learning classification identifies cerebellar contributions to early and moderate cognitive decline in Alzheimer's disease. Front Aging Neurosci 2020;12:524024.
[5] Liang KJ, Carlson ES. Resistance, vulnerability and resilience: A review of the cognitive cerebellum in aging and neurodegenerative diseases. Neurobiol Learn Mem 2020;170:106981.
[6] Toniolo S, Serra L, Olivito G, Marra C, Bozzali M, Cercignani M. Patterns of cerebellar gray matter atrophy across Alzheimer's Disease progression. Front Cell Neurosci 2018;12:430.
[7] Tomic JL, Pensalfini A, Head E, Glabe CG. Soluble fibrillar oligomer levels are elevated in Alzheimer's disease brain and correlate with cognitive dysfunction. Neurobiol Dis 2009;35(3):352–8.
[8] Pedroso JL, Braga-Neto P, Felício AC, Dutra LA, Santos WAC, do Prado GF, et al. Sleep disorders in machado-joseph disease: frequency, discriminative thresholds, predictive values, and correlation with ataxia-related motor and non-motor features. Cerebellum 2011;10(2):291–5.
[9] Song BJ, Zhu JC. A narrative review of cerebellar malfunctions and sleep disturbances. Front Neurosci 2021;15:590619.
[10] Zhang LB, Zhang J, Sun MJ, Chen H, Yan J, Luo FL, et al. Neuronal activity in the cerebellum during the sleep-wakefulness transition in mice. Neurosci 2020;36:919–31.
[11] Smith SM, Jenkinson M, Woolrich MW, Beckmann CF, Behrens TE, Johansen-Berg H, et al. Advances in functional and structural MR image analysis and implementation as FSL. Neuroimage 2004;23(Suppl 1):S208–19.
[12] Liang S, Wu S, Huang Q, Duan S, Liu H, Li Y, et al. Rat brain digital stereotaxic white matter atlas with fine tract delineation in Paxinos space and its automated applications in DTI data analysis. Magn Reson Imaging 2017;43:122–8.
[13] Xia M, Wang J, He Y, Csermely P. BrainNet Viewer: a network visualization tool for human brain connectomics. PLoS One 2013;8(7):e68910.
[14] Stoodley CJ, Schmahmann JD. Functional topography of the human cerebellum. Handb Clin Neurol 2018;154:59–70.
[15] Amore G, Spoto G, Ieni A, Vetri L, Quatrosi G, Di Rosa G, et al. A focus on the cerebellum: from embryogenesis to an age-related clinical perspective. Front Syst Neurosci 2021;15:646052.
[16] Baril AA, Martineau-Dussault MÈ, Sanchez E, André C, Thompson C, Legault J, et al. Obstructive sleep apnea and the brain: a focus on gray and white matter structure. Curr Neurol Neurosci Rep 2021;21:11.
[17] Assari S, Boyce S. Race, socioeconomic status, and cerebellum cortex fractional anisotropy in pre-adolescents. Adolescents 2021;1:70–94.
[18] Sotak CH. Nuclear magnetic resonance (NMR) measurement of the apparent diffusion coefficient (ADC) of tissue water and its relationship to cell volume changes in pathological states. Neurochem Int 2004;45(4):569–82.
[19] Ashburner J, Friston KJ. Voxel-based morphometry-the methods. Neuroimage 2000;11(6):805–21.
[20] Colloby SJ, O'Brien JT, Taylor J-P. Patterns of cerebellar volume loss in dementia with Lewy bodies and Alzheimer's disease: a VBM-DARTEL study. Psychiatry Res 2014;223(3):187–91.
[21] Zalesky A, Fornito A, Harding IH, Cocchi L, Yücel M, Pantelis C, et al. Whole-brain anatomical networks: does the choice of nodes matter? Neuroimage 2010;50(3):970–83.
[22] Park HJ, Friston K. Structural and functional brain networks: from connections to cognition. Science 2013;342:1238411.

[23] Greicius MD, Supekar K, Menon V, Dougherty RF. Restingstate functional connectivity reflects structural connectivity in the default mode network. Cereb Cortex 2009;19(1):72–8.
[24] Bai F, Shu Ni, Yuan Y, Shi Y, Yu H, Wu Di, et al. Topologically convergent and divergent structural connectivity patterns between patients with remitted geriatric depression and amnestic mild cognitive impairment. J Neurosci 2012;32(12):4307–18.
[25] Fischer FU, Wolf D, Scheurich A, Fellgiebel A. Altered whole-brain white matternetworks in preclinical Alzheimer's disease. Neuroimage Clin 2015;8:660–6.
[26] Muñoz-Moreno E, Tudela R, López-Gil X, Soria G. Early brain connectivity alterations and cognitive impairment in a rat model of Alzheimer's disease. Alzheimers Res Ther 2018;10:16.
[27] Bouix S, Pasternak O, Rathi Y, Pelavin PE, Zafonte R, Shenton ME, et al. Increased gray matter diffusion anisotropy in patients with persistent post-concussive symptoms following mild traumatic brain injury. PLoS One 2013;8(6):e66205.
[28] Lenfeldt N, Larsson A, Nyberg L, Birgander R, Forsgren L. Fractional anisotropy in the substantia nigra in Parkinson's disease: a complex picture. Eur J Neurol 2015;22(10):1408–14.
[29] Frost GR, Li Y-M. The role of astrocytes in amyloid production and Alzheimer's disease. Open Biol 2017;7(12):170228.
[30] Aviles-Reyes RX, Angelo MF, Villarreal A, Rios H, Lazarowski A, Ramos AJ. Intermittent hypoxia during sleep induces reactive gliosis and limited neuronal death in rats: implications for sleep apnea. J Neurochem 2010;112:854–69.
[31] Filippi M, Canu E, Gasparotti R, Agosta F, Valsecchi P, Lodoli G, et al. Patterns of brain structural changes in first-contact, antipsychotic drug-naive patients with schizophrenia. AJNR Am J Neuroradiol 2014;35:30–7.
[32] Koch K, Wagner G, Dahnke R, Schachtzabel C, Schultz C, Roebel M, et al. Disrupted white matter integrity of corticopontine-cerebellar circuitry in schizophrenia. Eur Arch Psychiatry Clin Neurosci 2010;260(5):419–26.
[33] Ratner V, Gao Y, Lee H, Elkin R, Nedergaard M, Benveniste H, et al. Cerebrospinal and interstitial fluid transport via the glymphatic pathway modeled by optimal mass transport. Neuroimage 2017;152:530–7.
[34] Demiral ŞB, Tomasi D, Sarlls J, Lee H, Wiers CE, Zehra A, et al. Apparent diffusion coefficient changes in human brain during sleep - Does it inform on the existence of a glymphatic system? Neuroimage 2019;185:263–73.
[35] Schmahmann JD. The cerebellum and cognition. Neurosci Lett 2019;688:62–75.
[36] Qi Z, An Y, Zhang M, Li HJ, Lu J. Altered cerebro-cerebellar limbic network in AD spectrum: a resting-state fMRI study. Front Neural Circuits 2019;13:72.
[37] Badea A, Wu W, Shuff J, Wang M, Anderson RJ, Qi Y, et al. Identifying vulnerable brain networks in mouse models of genetic risk factors for late onset Alzheimer's disease. Front Neuroinform 2019;13:72.
[38] Chen KT, Ho TY, Siow TY, Yeh YC, Huang SY. Individual cerebrocerebellar functional network analysis decoding symptomatologic dynamics of postoperative cerebellar mutism syndrome. Cereb Cortex Commun. 2022;3:tgac008.
[39] Drzezga A. The network degeneration hypothesis: spread of neurodegenerative patterns along neuronal brain networks. J Nucl Med 2018;59(11):1645–8.
[40] Hoenig MC, Bischof GN, Seemiller J, Hammes J, Kukolja J, Onur ÖA, et al. Networks of tau distribution in Alzheimer's disease. Brain 2018;141:568–81.
[41] Huijbers W, Mormino EC, Schultz AP, Wigman S, Ward AM, Larvie M, et al. Amyloid-β deposition in mild cognitive impairment is associated with increased hippocampal activity, atrophy and clinical progression. Brain 2015;138:1023–35.
[42] Lin C-Y, Chen C-H, Tom SE, Kuo S-H. Alzheimer's disease neuroimaging initiative. cerebellar volume is associated with cognitive decline in mild cognitive impairment: results from ADNI. Cerebellum 2020;19(2):217–25.
[43] Liu J, Zou G, Xu J, Zhou S, Qin L, Sun H, et al. State-dependent and region-specific alterations of cerebellar connectivity across stable human wakefulness and NREM sleep states. Neuroimage 2023;266:119823.
[44] Loschky SS, Spano GM, Marshall W, Schroeder A, Nemec KM, Schiereck SS, de Vivo L, Bellesi M, Banningh SW, Tononi G, Cirelli C. Ultrastructural effects of sleep and wake on the parallel fiber synapses of the cerebellum. Elife. 2022;11:e84199.
[45] Cunchillos JD, De Andrés I. Participation of the cerebellum in the regulation of the sleep-wakefulness cycle. Results in cerebellectomized cats. Electroencephalogr Clin Neurophysiol 1982;53:549–58.
[46] Schabus M, Dang-Vu TT, Albouy G, Balteau E, Boly M, Carrier J, et al. Hemodynamic cerebral correlates of sleep spindles during human non-rapid eye movement sleep. Proc Natl Acad Sci U S A 2007;104:13164–9.
[47] Xu W, De Carvalho F, Clarke AK, Jackson A. Communication from the cerebellum to the neocortex during sleep spindles. Prog Neurobiol 2021;199:101940.
[48] Um YH, Wang S-M, Kang DW, Kim N-Y, Lim HK. Subcortical and cerebellar neural correlates of prodromal alzheimer's disease with prolonged sleep latency. J Alzheimers Dis 2022;86(2):565–78.
[49] Reiman EM, Quiroz YT, Fleisher AS, Chen K, Velez-Pardo C, Jimenez-Del-Rio M, et al. Brain imaging and fluid biomarker analysis in young adults at genetic risk for autosomal dominant Alzheimer's disease in the presenilin 1 E280A kindred: a case-control study. Lancet Neurol 2012;11(12):1048–56.
[50] Jacobs HIL, Hopkins DA, Mayrhofer HC, Bruner E, van Leeuwen FW, Raaijmakers W, et al. The cerebellum in Alzheimer's disease: evaluating its role in cognitive decline. Brain 2018;141:37–47.
[51] Bruchhage MMK, Correia S, Malloy P, Salloway S, Deoni S. Machine learning classification identifies cerebellar contributions to early and moderate cognitive decline in Alzheimer's Disease. Front Aging Neurosci 2020;12:524024.
[52] Boucetta S, Salimi A, Dadar M, Jones BE, Collins DL, Dang-Vu TT. Structural brain alterations associated with rapid eye movement sleep behavior disorder in parkinson's disease. Sci Rep 2016;6:26782.